Translational Oncology 14 (2021) 101209

Contents lists available at ScienceDirect

Translational Oncology

journal homepage: www.elsevier.com/locate/tranon

Original Research

Combined metformin-salicylate treatment provides improved anti-tumor activity and enhanced radiotherapy response in prostate cancer; *drug synergy at clinically relevant doses*

Evangelia E. Tsakiridis [a,b,1], Lindsay Broadfield [a,b,1], Katarina Marcinko [a,b,1], Olga-Demetra Biziotis [a,c], Amr Ali [a,c], Bassem Mekhaeil [a,c], Elham Ahmadi [a,c], Kanwaldeep Singh [c], Aruz Mesci [e], Panayiotis G. Zacharidis [a,c], Alexander E. Anagnostopoulos [a,c], Tobias Berg [c], Paola Muti [c], Gregory R. Steinberg [a,b,f], Theodoros Tsakiridis [a,c,d,e,*]

[a] *Centre for Metabolism, Obesity and Diabetes Research, McMaster University, Hamilton, Ontario, Canada*
[b] *Department of Medicine, McMaster University, Hamilton, Ontario, Canada*
[c] *Department of Oncology, McMaster University, Hamilton, Ontario, Canada*
[d] *Department of Pathology and Molecular Medicine, McMaster University, Hamilton, Ontario, Canada*
[e] *Department of Radiation Oncology, Juravinski Cancer Center, 699 Concession Street, Hamilton, Ontario L8V 5C2, Canada*
[f] *Department of Biochemistry and Biomedical Sciences, McMaster University, Hamilton, Ontario, Canada*

ARTICLE INFO

Keywords:
AMPK
Lipogenesis
mTOR
HIF1a
Histone-H3
Xenografts

ABSTRACT

Background: There is need for well-tolerated therapies for prostate cancer (PrCa) secondary prevention and to improve response to radiotherapy (RT). The anti-diabetic agent metformin (MET) and the aspirin metabolite salicylate (SAL) are shown to activate AMP-activated protein kinase (AMPK), suppress de novo lipogenesis (DNL), the mammalian target of rapamycin (mTOR) pathway and reduce PrCa proliferation *in-vitro*. The purpose of this study was to examine whether combined MET+SAL treatment could provide enhanced PrCa tumor suppression and improve response to RT.

Methods: Androgen-sensitive (22RV1) and resistant (PC3, DU-145) PrCa cells and PC3 xenografts were used to examine whether combined treatment with MET+SAL can provide improved anti-tumor activity compared to each agent alone in non-irradiated and irradiated PrCa cells and tumors. Mechanisms of action were investigated with analysis of signaling events, mitochondria respiration and DNL activity assays.

Results: We observed that PrCa cells are resistant to clinically relevant doses of MET. Combined MET + SAL treatment provides synergistic anti-proliferative activity at clinically relevant doses and enhances the anti-proliferative effects of RT. This was associated with suppression of oxygen consumption rate (OCR), activation of AMPK, suppression of acetyl-CoA carboxylase (ACC)-DNL and mTOR-$p70^{s6k}$/4EBP1 and HIF1α pathways. MET + SAL reduced tumor growth in non-irradiated tumors and enhanced the effects of RT.

Conclusion: MET+SAL treatment suppresses PrCa cell proliferation and tumor growth and enhances responses to RT at clinically relevant doses. Since MET and SAL are safe, widely-used and inexpensive agents, these data support the investigation of MET+SAL in PrCa clinical trials alone and in combination with RT.

Abbreviations: PrCa, prostate cancer; MET, metformin; SAL, salicylate; MET + SAL, metformin and salicylate used together; RT, radiotherapy / ionizing irradiation with clinical radiotherapy units; DNL, de novo lipogenesis; mTOR, the mammalian target of rapamycin; mTORC1, mTOR complex 1; AMPK, AMP-activated protein kinase; LKB1, Liver Kinase B 1; $p70^{s6k}$, ribosomal p70 S6 kinase; ACC, acetyl-CoA carboxylase; TSC2, Tuberin Sclerosis Complex 2; 4EBP1, Eukaryotic Translation Initiation Factor 4E Binding Protein 1; HIF1α, hypoxia inducible factor 1; OxPhos, oxidative phosphorylation; OCR, oxygen consumption rate; ECAR, Extracellular Acidification Rate; P-H3, phosphorylated histone H3; IHC, immunohistochemistry.

* Corresponding author at: Centre for Metabolism, Obesity and Diabetes Research, Hamilton, Ontario, Canada.
E-mail address: theos.tsakiridis@hhsc.ca (T. Tsakiridis).

[1] These authors contributed equally to this work.

https://doi.org/10.1016/j.tranon.2021.101209
Received 14 June 2021; Received in revised form 3 August 2021; Accepted 18 August 2021
Available online 31 August 2021

Introduction

Prostate cancer (PrCa) is the most commonly diagnosed cancer in men in the western world, with over 200,000 patients diagnosed in North America alone in 2020 [1,2]. Radiation therapy (RT) is a key therapeutic modality for all stages of PrCa but prostate tumors are relatively resistant to this treatment. Dose-escalated RT improves local disease control but is associated with significant bladder and bowel toxicity [3,4], highlighting the need for effective radio-sensitizers.

In preclinical studies, targeting tumor metabolism, with agents such as mitochondria oxidative phosphorylation (OxPhos) chain inhibitors [5], suppresses cancer cell growth and improves tumor response to local and systemic therapies [6]. Metformin (MET), a widely used first-line type 2 diabetes drug, is a mild OxPhos inhibitor [7,8], attenuates growth and sensitizes epithelial tumors, including PrCa, to cytotoxic therapy [9,10–13]. Retrospective clinical studies observed reduced cancer incidence and improved tumor control with MET use [14–17] and triggered pre-clinical and clinical studies in a variety of tumor types in recent years [6]. However, it remains controversial whether MET can safely reach circulating concentrations required for anti-tumor activity. Apart from one study that showed anti-tumor activity with micromolar (μM) doses of MET [18], most pre-clinical reports in PrCa detected anti-tumor and radiation-sensitizing activity only at clinically unattainable millimolar (mM) concentrations of the drug [11–13].

Dowling et al. [19], found that intraperitoneal injection of MET (125 mg/kg) in mice can lead to transient mean serum MET concentration of 14 μM (range 61–28 μM) and maintain an average serum concentration of 77 μM (range 41.6–99.0 μM) for about 1 h. On the other hand, supply of MET in the animal drinking water at 5 mg/ml (250–300 mg/kg/day based on water consumption of ~2 ml per day and body weight of 30 gr) led to average serum MET of 34 μM (range 2.3–126.2 μM) and average tumor concentration of 32 μM (9.1–55.7 μM). These values are similar to concentrations that are observed in human serum (~4.5–38.8 μM, depending on renal function) achieved with oral MET intake of 1500–3000 mg/day [20].

Mitochondria OxPhos complex I inhibition by MET activates AMP-activated kinase (AMPK) [6,21,22], an evolutionarily conserved enzyme that responds to energy and genomic stress signals [6,21,22]. AMPK is a heterotrimeric enzyme composed of α−, β− and γ-subunits, the latter containing a regulatory ADP/AMP binding domain allowing for allosteric activation of AMPK [22,23]. α-subunit T172 is phosphorylated by upstream kinases such as the tumor suppressor Liver Kinase B 1 (LKB1) [22], while ADP/AMP binding to γ-subunit reduces de-phosphorylation on that site [24]. OxPhos inhibition, with agents like MET, reduces ATP synthesis and enhances ADP and AMP binding on the AMPK γ-subunit. Activated AMPK triggers energy conservation through inhibition of biosynthetic events, including lipogenesis, protein synthesis and cellular growth [25–28]. These are mediated by direct inhibitory phosphorylation events on acetyl-CoA carboxylase (ACC), a rate limiting step in de novo lipogenesis (DNL) [26], Tuberin Sclerosis Complex 2 (TSC2) [29] and the regulator of the mammalian Target of Rapamycin complex 1 (mTORC1) Raptor [30], which regulate protein synthesis. We found that MET mediates tumor suppression and radio-sensitization in lung cancer models at low μM drug doses [9]. However, in PrCa cells were resistant to MET's anti-tumor activity (Storozhuk et al. [9] *supplemental data*), suggesting that additional metabolic targeting may be needed.

The widely-used anti-inflammatory agent aspirin is linked to reductions in PrCa-related deaths [13,14]. Retrospective clinical studies have suggested that aspirin is associated with improved response to radiotherapy (RT) [15,16]. After ingestion, aspirin is rapidly metabolized to salicylate (SAL) by carboxy-esterases, a step that enhances its circulating concentration and half-life [31]. SAL interacts with the Ser108 residue of the β-subunit, leading to allosteric activation of AMPK and prevention of de-phosphorylation of the Thr172 residue on the α-subunit, yielding maximal kinase activity [32]. Therefore, aspirin has been considered for cancer prevention and improvement in efficacy of standard therapy. However, long term treatment with high doses of aspirin (acetyl-salicylate) can lead to bleeding events through its acetyl-group that is cleaved and inhibits prostaglandin synthesis (see [31] for review). To address this concern, oral delivery of salsalate, a SAL dimer/prodrug, can be used, to achieve safely SAL serum concentrations up to 900 μM [31,32]; sufficient to activate AMPK.

We observed that combined MET + SAL treatment has improved anti-proliferative activity in lung and prostate cancer cell lines in-vitro, compared to each agent alone [33], but whether this therapy could be effective *in-vivo* alone or in combination with RT was not studied. Further, we reported the tumor suppressive efficacy of SAL and salsalate in combination with RT in PrCa models [34], however, salsalate alone did not suppress tumor growth in non-irradiated xenografts.

The purpose of the present study was to examine whether combination of clinically relevant doses of MET and SAL can provide improved anti-proliferative and tumor suppressive activity, compare to each agent alone, in untreated and irradiated models of human PrCa.

Materials and methods

Cell lines

Prostate cancer cells (PC3 and 22RV1) were obtained from the American Type Culture Collection (ATCC). The DU145 cells were provided by Dr. Stanley Liu, University of Toronto. Cells were grown in Roswell Park Memorial Institute (RPMI) medium supplemented with 1% antibiotic–anti-mycotic and 10% FBS (Gibco).

Materials

Metformin, Salicylate and all standard chemicals were obtained from Sigma Aldrich. All antibodies (AMPK, p-AMPK T-175, ACC, p-ACC-S-79, H3 and P-H3-S10, HIF1a, $p70^{S6k}$, P-$p70^{S6k}$-T389, P-S6-S235/236, P-4EBP1-T37/46 and β-actin) were purchased from (Cell Signaling Technology). Biotinylated goat-anti-rabbit secondary antibody conjugated with streptavidin peroxidase and Nova Red were from Vector labs (Burlingame, CA).

Cell treatments

All cells were maintained at 37 °C, 5% CO_2 and treated with indicated concentration of metformin (MET), salicylate (SAL) and radiotherapy (RT). All drug treatments were performed 4–24 h prior to delivery of RT using established dosimetry.

Proliferation assays

Cells were seeded in 96-well plates at 500 cells/well and allowed to adhere overnight. After drug and RT treatments cells were incubated until control wells reached 80% confluence (5–6 days post treatment initiation), defined as experimental endpoint. Cells were washed, fixed with 10% formalin for 10 min, stained with 0.5% Crystal Violet stain in 20% MeOH for 10 min and dried overnight. Stain was solubilized followed by an absorbance reading at 570 nM yielding cell density measurements.

Clonogenic assays

Approximately 500–8000 cells were seeded into 12-well plates, allowed to adhere overnight and subsequently treated with indicated doses of drugs and RT. After 7 days, cells were fixed with crystal violet and viable colonies (> 50 cells) were counted.

Lipogenesis assay

Cells were treated with drugs for 8 h before RT followed by 48 h incubation. Then cells were radio-labelled with ^{3}H-sodium acetate (10 μCi/ml, PerkinElmer) and unlabeled sodium acetate (0.5 mM, Sigma-Aldrich) for 4 h, washed, scraped and subjected to chloroform-methanol lipid extraction, as described [24]. Lipid synthesis values were normalized to DNA content to account for the anti-proliferative effects of treatments.

Xenograft experiments

Five-week old male BALB/c-Nude mice (Charles-River Laboratories) were housed in a pathogen-free facility with ad libitum access to chow diet and water. PC3 cells (1×10^6) were grafted subcutaneously into the mouse flank. Tumor length and width were measured at the indicated times with a caliper to determine tumor volume using the formula: 0.5* (W^2xL; W:width, L:length). Animals were treated as described in Fig. 3 legend. When control animals reached end-point, all animals were sacrificed (7 weeks after drug treatment initiation). Tumor volumes were measured directly, and tumors were fixed (10% formalin, 48 h) and paraffin embedded (FFPE). All animal procedures were approved by an institutional Animal Ethics Research Board.

Immunohistochemistry (IHC)

FFPE tumors were sectioned in 5 μm thick sections. Sections were deparaffinized in xylene and ethanol, followed by endogenous peroxidase removal, and heat antigen retrieval in citrate buffer. Tissues were blocked in 10% goat serum (Vector) and incubated with either non-specific (negative control) serum or anti-phosphorylated Histone H3 (Ser10) rabbit monoclonal antibody was used at 1:200 dilution, followed by 1:500 biotinylated goat-anti-rabbit secondary antibody streptavidin peroxidase, and developed using Nova Red. Hematoxylin was used as counter stain.

Immunoblotting

Cells were seeded in 6-well plates, treated with indicated doses of drugs and RT and incubated for 48 h. Then cells were washed and lysed, subjected to electrophoresis (SDS-PAGE), immunoblotting and imaging using a Vilber Fusion-FX7 imaging system (Marne-la-Vallée, France).

Oxygen consumption rate (OCR)

OCR and Extracellular Acidification Rate (ECAR) were measured in cells seeded at 20,000 per well, treated with the indicated doses of drugs and RT, and analyzed 48 h later using the Agilent Technologies Seahorse XFe96 extracellular flux analyzer system (Santa Clara, CA). Inhibitors: oligomycin, FCCP, rotenone and antimycin A were utilized at concentrations of 1.5 μM, 1 μM and 0.5 μM for both rotenone and antimycin A, respectively.

Statistical analysis

Results were analyzed using two-way ANOVA and multiple comparison by Tukey post hoc test, using GraphPad Prism software (v.8, San Diego, CA), unless indicated otherwise. Student's *t*-test or one-way ANOVA were used in limited situations as indicated in figure legends. Significance was accepted at $P \leq 0.05$. P value ≤ 0.05, ≤ 0.01, ≤ 0.001 and ≤ 0.0001 indicated by 1, 2, 3 and 4 symbols, respectively. Significant differences within RT doses and between RT doses are depicted. * indicating significance compare to control within the same RT group, # between drug treatments within the same RT treatment and $ indicating differences between RT doses. Combination Index (CI) analysis was pursued with the Chou-Talalay method, using the CompuSyn software (ComboSyn Inc, Paramus, NJ) [35].

Results

Effects of ionizing irradiation (RT), metformin (MET), salicylate (SAL) and combinations on PrCa cell growth

Proliferation and clonogenic survival assays were performed after exposing PC3, DU145 and 22RV1 PrCa cells to ionizing radiation (0–8 Gy) using clinical radiotherapy units (RT), MET or SAL doses of 25–1000 μM alone or drug and RT combinations. Fig. 1A illustrates the responsiveness of PrCa cells to RT. It confirms the known resistance of DU145 cells and higher sensitivity of 22RV1 cells to ionizing radiation [36,37]. We did not detect anti-proliferative activity with MET doses of less than 100μM in any of the three cell lines (not shown). In non-irradiated cells, MET at 100μM caused minor inhibition of proliferation (4.8–11.7%), which became significant only at higher doses (500–1000 μM, Fig. 1B–D). DU145 cells showed greater response to high dose MET (1000 μM) but PC3 cells showed the greatest sensitivity to 100 μM MET (see Fig. s1A for a clear comparison of MET effects amongst the three cell lines). Similar results were obtained with clonogenic survival assays where 100 μM MET caused a 22.7% reduction in PC3 cell survival increasing to 60% at 1000μM (Fig. s1B). This suggested that our proliferation assays accurately represent the oncogenic potential of PrCa cells. Addition of MET (100–1000 μM) to

PC3, DU145 and 22RV1 cells treated with increasing doses of RT (2–8 Gy) demonstrated only minimal additional anti-proliferative capacity (10% or less) of 100μM MET beyond that achieved with RT alone (Fig. 1B–D). Only high dose MET (500–1000 μM) provided greater suppression of proliferation (~20–25%) in PC3 and DU145 cells treated with 2 or 4 Gy RT, but this benefit was also eliminated at higher RT doses (8 Gy). These data suggest that therapeutically relevant concentrations of MET are unlikely to enhance the effects of RT.

Based on our earlier work with salicylate (SAL) [33], we focused subsequent analysis on clinically relevant drug combinations of MET at 100μM and SAL doses in the range of 250–1000 μM. Addition of SAL (500 μM) to low dose MET (100 μM) provided greater inhibition of proliferation in non-irradiated and irradiated (2 Gy) PC3 PrCa cells, compared to each drug alone (Fig. 2A). In DU145 cells, MET or SAL induced minor trends for inhibition of proliferation but this reached statistical significance in MET + SAL treated cells. (Fig. 2B). Similar increased suppression of proliferation was obtained in cells irradiated with 2 Gy. In androgen-sensitive non-irradiated 22RV1 cells SAL (500 μM), but not MET (100 μM), significantly suppressed proliferation (Fig. 2C). No clear improvement could be produced by the drug combination in non-irradiated cells but in 2 Gy irradiated cells MET + SAL was able to suppress significantly proliferation beyond the effect of RT alone. Of note, we have obtained similar results in experiments with the androgen-responsive LnCap PrCa cells (Fig. s2). Overall, combined treatment with low dose MET + SAL provided improved suppression of proliferation in a variety of androgen-sensitive and in-sensitive non-irradiated PrCa cells and cells treated with 2 Gy RT. Further, improvements in suppression of proliferation can be achieved with addition of higher doses of SAL in the MET + SAL combination. We observed increased suppression of proliferation in non-irradiated and 2 Gy irradiated PC3, DU145 and 22RV1 cells by increasing SAL dose to 1000 μM, a concentration only slightly higher than 900μM that is achieved *in-vivo* without increased toxicity[31,32](Fig.s3). Nevertheless, to remain within easily achievable doses, we chosen to pursue the majority of our studies with the 100μM MET + 500 μM SAL combination.

To verify whether the anti-proliferative effects of MET, SAL and MET+SAL combination reflect effects on PrCa oncogenic potential, we performed clonogenic survival assays with isomolar drug dose-escalation treatments (25–1000 μM) without or with irradiation (2 Gy) (Fig. 2D). MET and SAL independently supressed clonogenic survival at 100 μM or greater doses. However, combined equimolar MET +

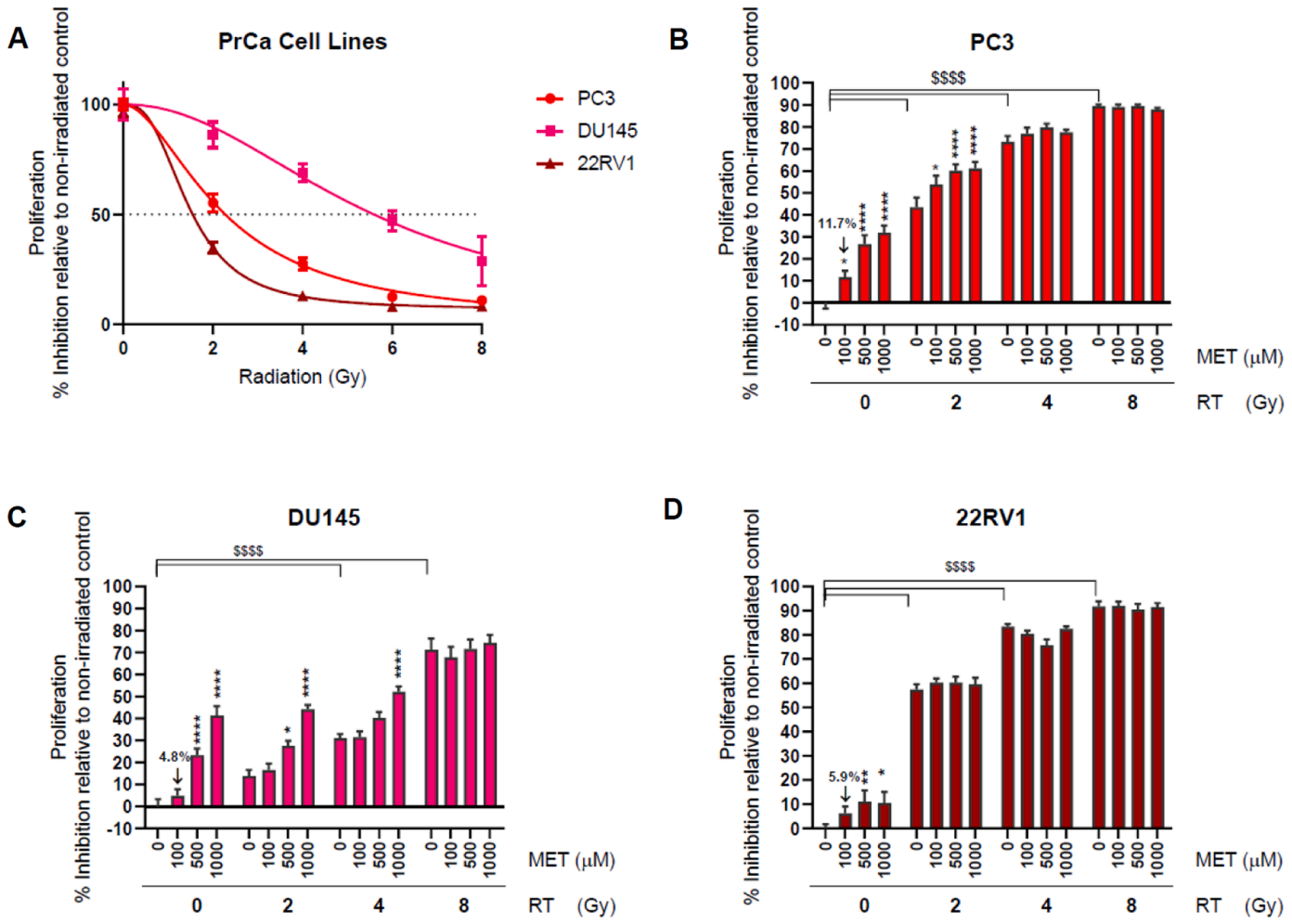

Fig. 1. Response of PrCa cells to Metformin (MET) and radiotherapy (RT). PC3, DU-145 and 22RV1 cells were subjected to proliferation assays after treatment with the indicated doses of RT, MET or combinations. (A) PrCa cell response to RT (0–8 Gy). Anti-proliferative efficacy MET in PC3 (B) DU-145 (C) and 22RV1 (D) cells treated with RT (0–8 Gy). *: $P < 0.05$, **: $P < 0.01$, ****/$$$$: $P < 0.0001$.

SAL treatment demonstrated inhibition of proliferation at concentrations as low as 50 μM in non-irradiated cells. In irradiated PC3 cells (2 Gy) SAL single agent tended to suppress clonogenic survival at 25–100 μM but demonstrated significant efficacy at doses of 50 μM or higher when combined with MET. Combination Index (CI) analysis with the Chou-Talalay method [35] demonstrated clear synergy between MET and SAL in doses of 25–250 μM in non-irradiated cells (Fig. 2E) and up to 100 μM in irradiated cells with antagonism developing at higher equimolar doses (Fig. 2F).

Effects on PrCa xenograft growth

To confirm whether the MET + SAL combination can provide improved tumor suppression in-vivo we investigated the effects of single drugs (MET or SAL) and the combination in non-irradiated and irradiated PC3 xenografts. Fig. 3A, shows that untreated tumors took a period of 10 weeks (70 days) to reach endpoint (average 8.0-fold growth compared to baseline). MET addition to drinking water had no significant effect on tumor growth. A small reduction in average tumor volume at endpoint evaluation was not statistically significant (NS)) (average 66.2% of control, Fig. 3A). Despite the anti-proliferative activity detected in-vitro with SAL treatment, addition of salsalate alone (a precursor of SAL) to animal diet had no detectable anti-tumor efficacy as a single agent in non-irradiated PC3 xenografts (98.3% of control). Addition of salsalate diet to MET-treated mice resulted in clear trends for tumor growth suppression, approaching statistical significance (54.3% of control, $P = 0.052$) (Fig. 3A). RT (10 Gy) alone suppressed tumor growth almost completely for 4 weeks. Tumors began recovering after 57 days and reached an average 23.2% of control (2.2-fold growth compared to baseline) at endpoint. Tumor growth did not recover in MET-treated irradiated animals (MET + RT). It stabilized at 90% of the pre-treatment value at 5 weeks, and remained unchanged until endpoint (smaller compared to RT-alone treated tumors, $P = 0.031$). Salsalate also prevented recovery from RT-induced tumor suppression (SAL + RT group). However, MET + SAL therapy of irradiated tumors (MET + SAL + RT group) further reduced tumor volumes, compared to MET + RT or SAL + RT groups, reaching higher statistical significance at endpoint, compared to RT alone group (33.1% of pre-treatment volume, $P = 0.0013$ compared to RT).

At endpoint, tumors were resected from animals, direct 3-dimentional volume measurements were taken and tumors were fixed for IHC analysis. *Ex-vivo* volumes (Mean ± SE in mm^3) for non-irradiated tumors were: Control: 1050 ± 203, MET: 650 ± 89, SAL: 982 ± 187, MET + SAL: 536 ± 216 [$P = 0.13$], compared to Control: 410 ± 120, MET: 170 ± 41 [$P = 0.117$], SAL: 178 ± 23 [$P = 0.08$] and MET+SAL: 85 ± 28 [$P < 0.05$] for the irradiated tumors (P values compared to control tumors within the same group).

Regulation of DNA replication markers

Tumors were subjected to IHC analysis using an anti-phosphorylated histone H3 (P-H3) specific antibody to assess the proportion of tumor

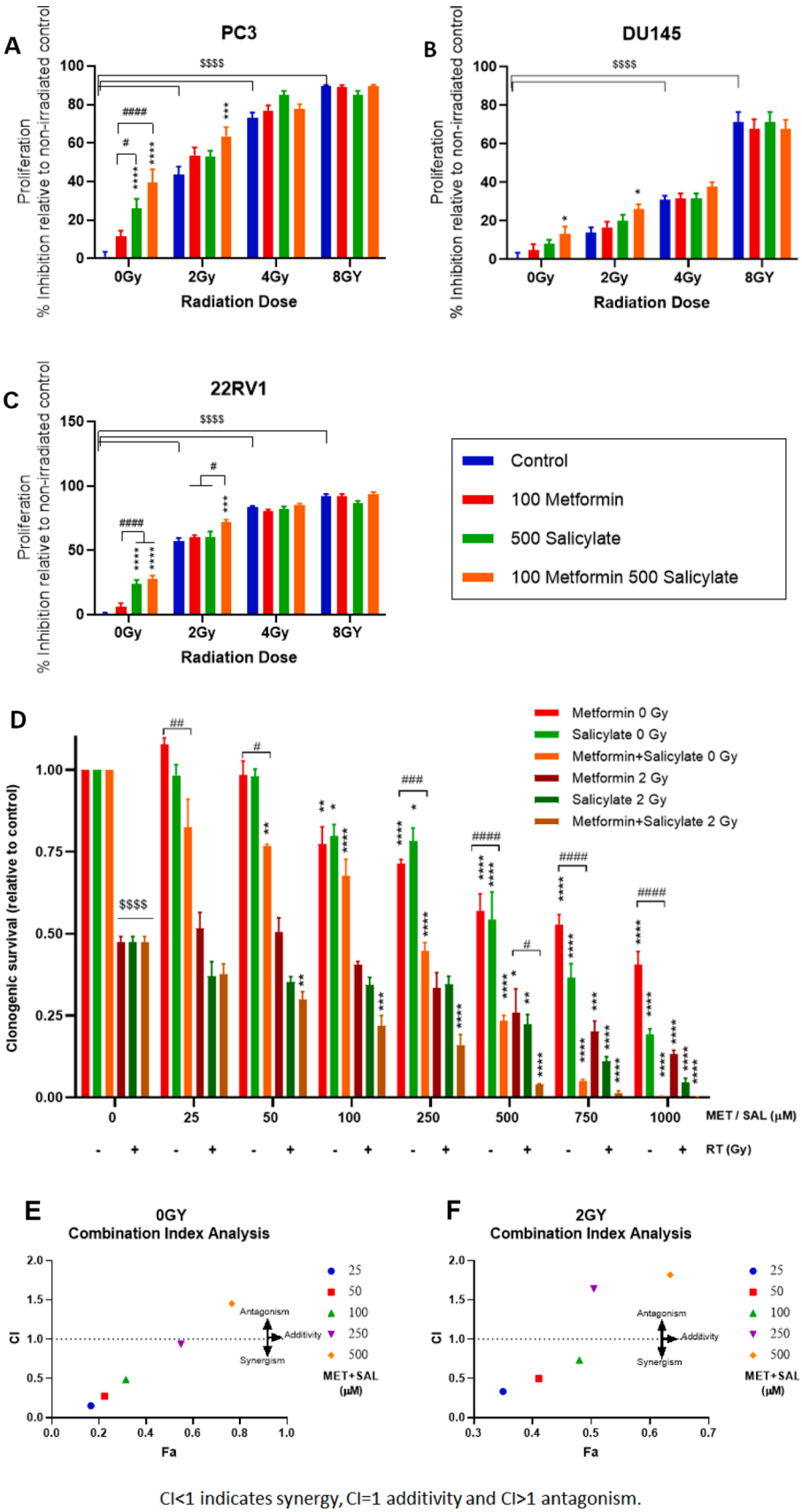

Fig. 2. Combined metformin (MET) + salicylate (SAL) treatment without or with radiotherapy (RT): effects on proliferation and clonogenic survival. PC3 (A, D, E, F) DU-145 (B) or 22RV1 (C) cells were treated with the indicated doses of MET, SAL or MET+SAL, with or without RT (2–8 Gy) and were subjected to proliferation (A–C) or clonogenic survival analysis assays (D). Clonogenic survival was evaluated after equimolar dose escalation (0–1000 μM) of MET and SAL treatment without or with 2 Gy RT (D). Clonogenic survival results were subjected to combination index (CI) analysis for non-irradiated (E) and irradiated (F) cells. CI is plotted against the affected fraction (Fa). */#: $P < 0.05$, **/##: $P < 0.01$, ***/###: $P < 0.001$, ****/####/$$$$: $P < 0.0001$.

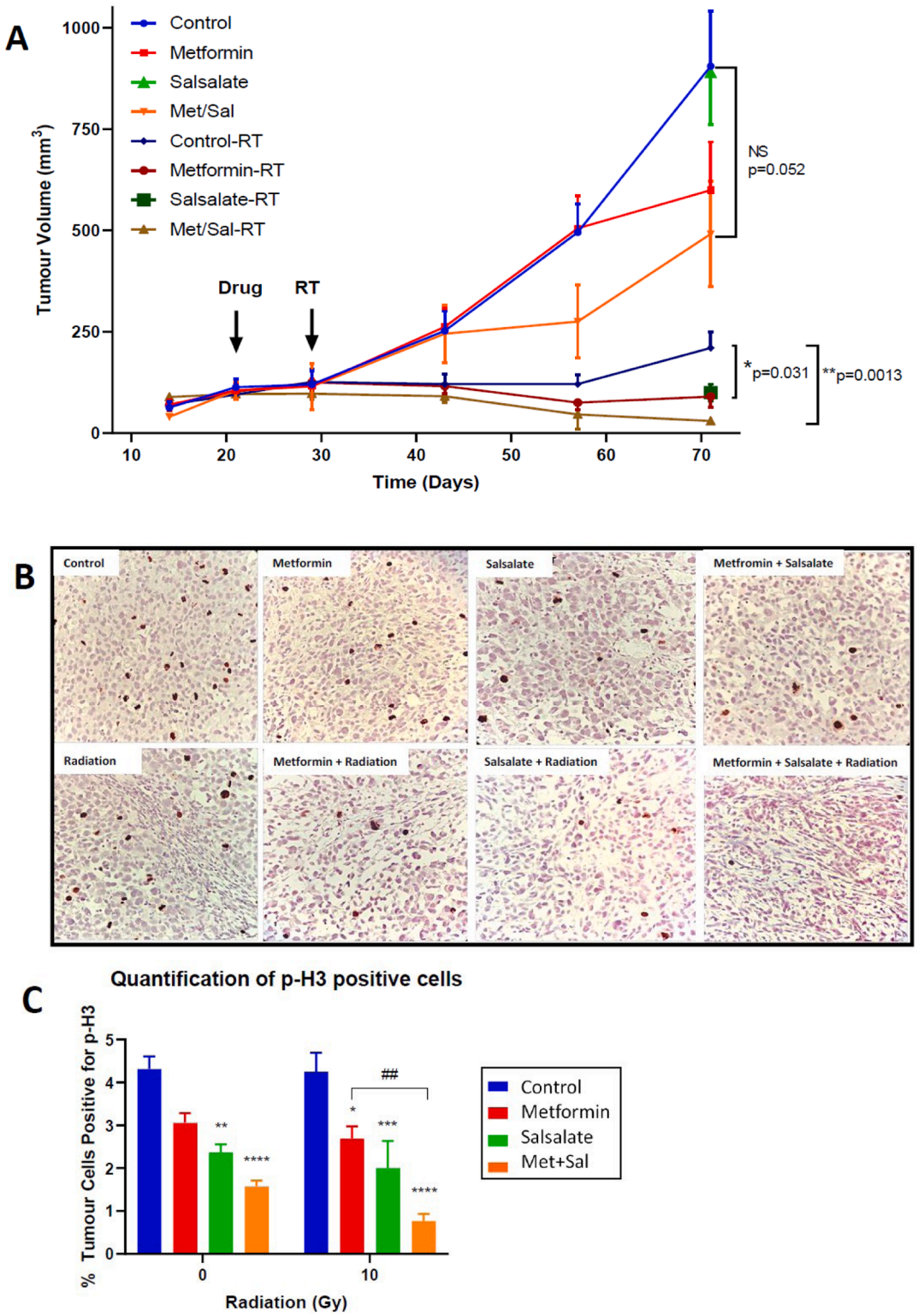

Fig. 3. Metformin and Salsalate combination mediates increased tumor suppression and inhibition of DNA replication in PrCa xenografts. PC3 xenografts were generated as described in Methods and assigned in groups to receive either vehicle, MET, Salsalate or the Metformin (Met) and Salsalate (Sal) combination without or with RT (single fraction of 10 Gy given 1 week after initiation of drug therapy). Metformin treatment was provided via the drinking water. The concentration was adjusted bi-weekly to achieve delivery of a dose of 250 mg/kg/day and salsalate was incorporated into the chow diet at 2.5 g/kg. Six animals were assigned per group. (A) Tumor growth kinetics: average volume estimates obtained using hand caliper measurements as described in Methods. Mean ± SEM for SAL- and SAL + RT-treated tumors are indicated only at the final evaluation. (B) Representative images of immunohistochemistry analysis of each condition using anti-phosphorylated histone H3 (P-H3) antibody (see Fig. s1 for P-H3 magnified and for negative control images). (C) For each treatment, areas were quantified for% of cells positive the P-H3 (number nuclei stained positive for P-H3 out of 100) and average values (Mean±SE, $N = 10$) were plotted. NS: non-significant, */#: $P < 0.05$, **/##: $P < 0.01$, ***: $P < 0.001$, ****: $P < 0.0001$.

cells undergoing DNA replication (see Methods). Fig. 3B shows representative images of tumor sections and illustrates the value of P-H3 as a specific marker of DNA replication and identifies cells progressing through cell cycle (see magnified and negative control images in Fig. s4). MET and Salsalate decreased the number of P-H3 positive nuclei in PC3 xenografts and combined treatment significantly enhanced this effect (Fig. 3C). Despite the substantial reduction in tumor volume in response to RT treatment alone, the number of P-H3 foci detected in those tumors (which received RT six weeks before resection) was similar to untreated tumors. Importantly, drug treatments mediated similar but quantitatively higher reduction of P-H3 foci in irradiated tumors. The MET + Salsalate + RT-treated group showed the lowest ratio of P-H3 positive nuclei, consistent with the maximal tumor growth inhibition observed (Fig. 3A).

Modulation of mitochondria respiration

Given that both MET and SAL inhibit OxPhos complex I[8,31], we examined OCR and ECAR rates in PC3 cells. The Seahorse extracellular flux analyzer data illustrate basal, OxPhos-dependent ATP-linked, maximal and non-mitochondria respiration rates (Fig. 4A,B, see also Fig. s5A for illustration of components of mitochondria respiration). Then OCR values corresponding to non-mitochondria oxygen consumption and proton leak for each treatment condition were subtracted and basal respiration rates are plotted as change with treatments relative to control in non-irradiated cells (value of 1.00, Fig. 4C). In non-irradiated cells MET (100 μM) and SAL (500 μM) alone caused minor changes to basal OCR (< 5%), relative to untreated control. However, combined MET +SAL treatment resulted in significant suppression of basal OCR (12.2%, $P < 0.05$) compared to control and MET treated cells

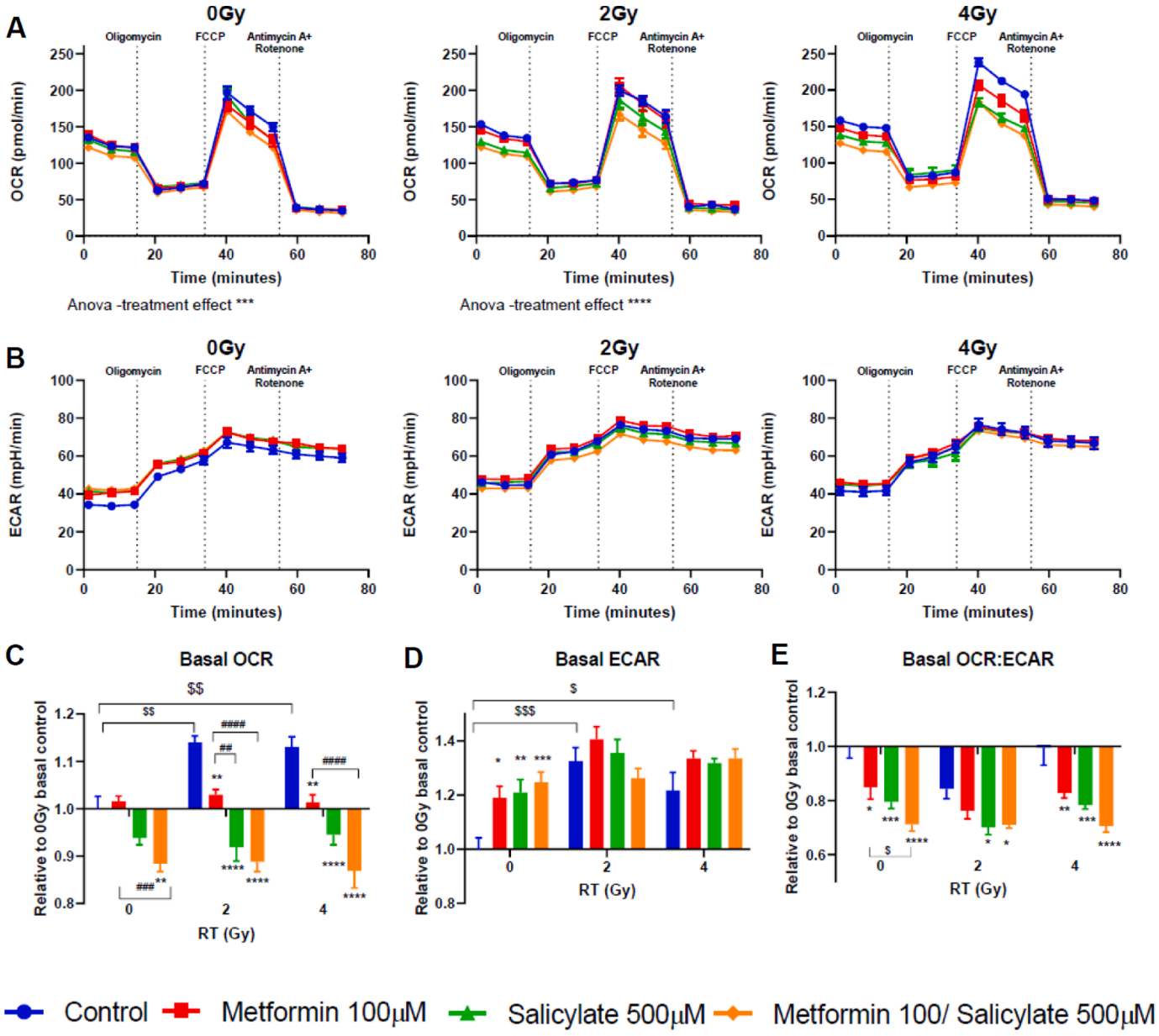

Fig. 4. Effects of drug and radiation treatments on oxygen consumption rate (OCR) and extracellular acidification rate (ECAR) in PC3 PrCa cells. Cells treated with the indicated drug doses and combinations 24 h after seeding, were subjected to radiation (0, 2 or 4 Gy) 24 h later. After 48 h incubation, cells were subjected to OCR and ECAR analysis, as described in Methods. (A) OCR and (B) ECAR curves were plotted for non-irradiated and irradiated (2–4 Gy) cells, respectively. Effects of drug and RT treatments on basal OCR (C), basal ECAR (D) and basal OCR/ECAR ratio (E) rates were plotted as changes relative to untreated control cells. */#/$: $P < 0.05$, **/##/$$: $P < 0.01$, ***/$$$/###: $P < 0.001$, ****/$$$$/####: $P < 0.0001$.

($P < 0.01$) (Fig. 4A,C). Small but statistically significant increases in ECAR were observed with single drug and combined MET+SAL treatments (Fig. 4B). Importantly, RT 2 or 4 Gy alone increased significantly basal (11.4%, 11.3%, $P < 0.01$) and maximal (8.4, 21%, $P < 0.01$) OCR rates and ECAR ($P \leq 0.001$ and $P \leq 0.05$, respectively) rates in PC3 cells (Fig. 4A–D and Fig. s3B–D). In irradiated cells MET and SAL provided significant suppression of OCR (basal and maximal rates), which increased further significantly with MET + SAL treatment (Figs. 4 and s5). The extracellular acidification rate (ECAR) did not change consistently with drug treatments in irradiated cells (Fig. 4D). Importantly, the

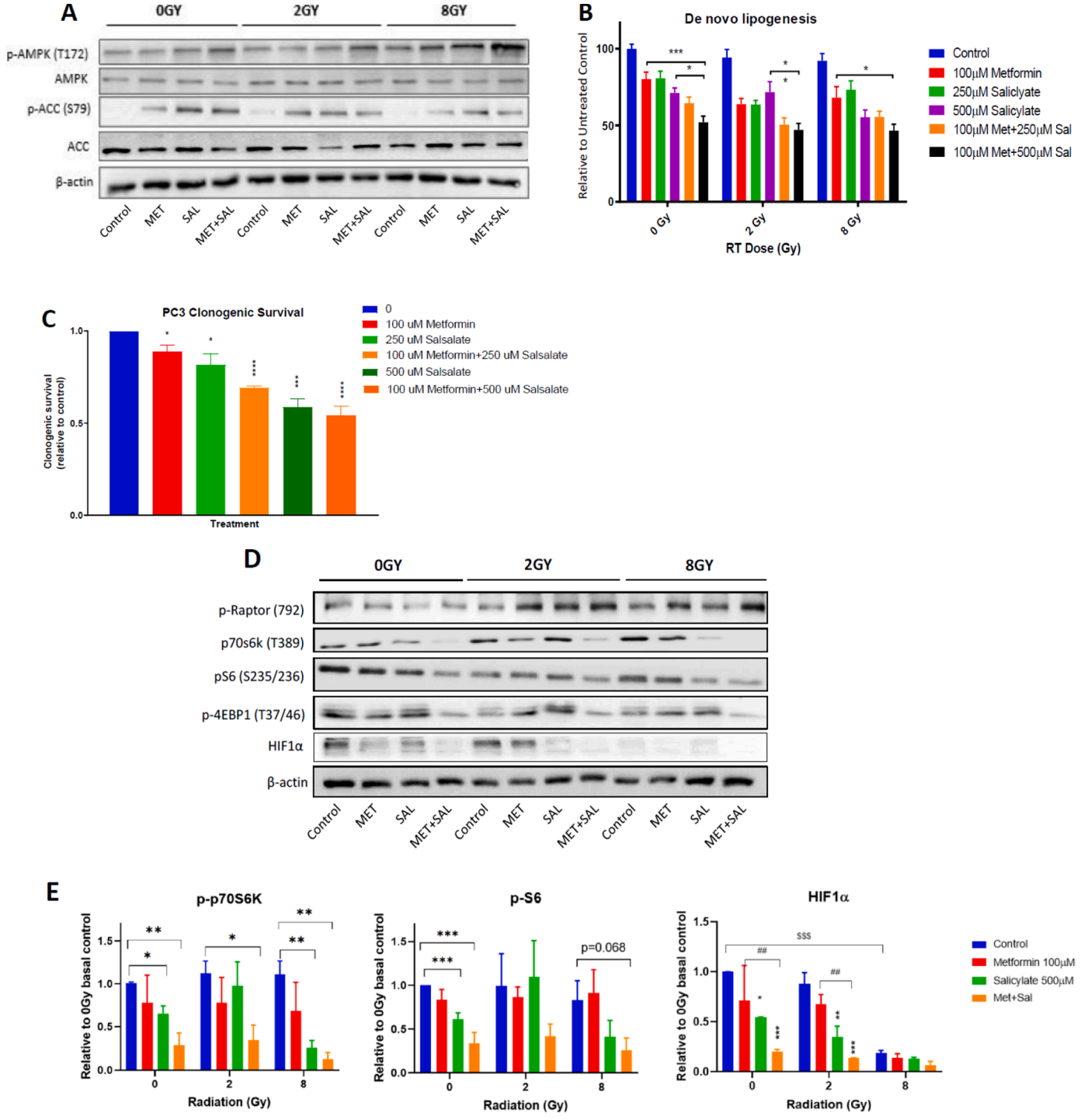

Fig. 5. Regulation of AMPK-ACC axis and de-novo lipogenesis (DNL). Cells subjected to drug and RT treatments were allowed to incubate for an additional 48 h before analysis with immunoblotting, and lipogenesis assays. (A) Representative immunoblots from 3 independent experiments analyzing the levels of phosphorylated and total AMPK alpha subunit and ACC1/2. (B) DNL values were normalized to proliferation (DNA stain) values for each condition. (C) Results of clonogenic survival assays from cells treated with the indicated doses and combinations, as described in Methods. Statistical analysis in this section (C) specifically was performed with one-way ANOVA. (D) Representative immunoblots from 3 to 4 independent experiments analyzing the levels of phosphorylated-Raptor, -p70^{S6k}, -S6 and −4EBP1 and total HIF1α and β-actin levels. Statistical analysis in this section (D) was performed with Student's *t*-test for p-p70^{S6k} and p-S6 and two-way ANOVA for HIF1α. (E) Quantification of results from 3 to 4 experiments for phosphorylated p70^{S6k}, S6 and total HIF1α levels. *: $P < 0.05$, **/##: $P < 0.01$, ***/$$$: $P < 0.001$, ****: $P < 0.0001$.

OCR/ECAR ratio, an index of the cellular metabolic stress, was inhibited in an increasing fashion by MET, SAL and more so by the combination (MET + SAL) (Fig. 4E) and was similar in non-irradiated and irradiated cells.

Effects on AMPK-ACC axis and de-novo lipogenesis (DNL)

To evaluate the impact of metabolic stress induced by drug treatments and RT, we analyzed the cellular levels of total and phosphorylated AMPK and ACC, the latter of which is a specific marker of cellular AMPK activity that measures both covalent and allosteric activation. While MET (100 μM) did not produce a detectable increase of P-AMPK levels except in cells treated with 8 Gy, it enhanced ACC phosphorylation in both control and irradiated cells, indicating increased AMPK activity despite its unchanged phosphorylation status (Fig. 5A). Similar effects were mediated by SAL (500 μM) treatment. Combined MET + SAL treatment enhanced P-AMPK levels in non-irradiated and irradiated cells, compared to each treatment alone (Fig. 5A), while ACC phosphorylation remained at similar levels. Consistent with these results, MET (100 μM) and SAL (250–500 μM) mediated increasing suppression of de novo lipogenesis (DNL) that was higher with combined treatments (Fig. 5B). Consistent with observations that the anti-proliferative effects of MET, SAL and MET + SAL are dependent on DNL [33], we found a parallel and equivalent suppression of PC3 clonogenic survival with the same drug treatments (Fig. 5C). DNL rates, normalized to DNA content, were similar in non-irradiated and irradiated (2 and 8 Gy) cells, illustrating that the suppression of DNL is independent of RT (Fig. 5B).

Regulation of the mTORC1-HIF1α pathway

MET, SAL and combined treatment mediated increased phosphorylation of Raptor Ser792, an established target of AMPK. This was more clearly detected in irradiated cells (Fig. 5D). MET (100μM) and SAL (500 μM) provided inconsistent inhibitor effects on the cellular levels of phosphorylated $p70^{S6k}$, S6 and 4EBP1 but MET + SAL achieved that consistently (Fig. 5D,E).

Importantly, MET and SAL suppressed the levels of HIF1α but the MET + SAL combination dramatically suppressed HIF1α levels in non-irradiated and 2 Gy RT treated cells.

Unlike the other mTORC1 mediators, HIF1α expression levels were suppressed by high dose RT (8 Gy) alone (Fig. 5D,E).

Fig. 6 illustrates a model summarizing our observations on the molecular mechanisms involved in the improved anti-tumor efficacy of MET + SAL treatment alone and in combination with RT, including targeting of cellular metabolism, AMPK activation, DNL suppression and inhibition of the mTOR-$p70^{S6k}$-S6/4EBP1 and HIF1α pathways.

Discussion

The main aim of this study was to examine whether combined treatment with clinically relevant doses of MET and SAL can provide improved anti-tumor efficacy, compared to each drug alone, in non-irradiated and irradiated models of PrCa.

Based on clinical observations discussed above[20], we determined that in-vitro observations made with MET concentrations higher than 100 μM have limited therapeutic relevance. For that, in agreement with earlier studies [19], we limited the oral MET delivery in our animal xenograft model to 250 mg/kg/day, which elicits mouse serum MET levels comparable to those obtained in patients treated with standard doses of MET [20]. At 100 μM MET mediated minimal suppression of proliferation and clonogenic survival in a variety of androgen sensitive and in-sensitive PrCa cells. This was consistent with limited inhibition of mitochondria OxPhos, the ACC-DNL and mTOR-HIF1α pathways (Figs. 2,5,6). *In-vivo*, oral MET also failed to suppress PrCa xenograft growth when used alone. Therefore, at clinically attainable doses, MET has no significant anti-tumor efficacy in PrCa models as a single agent and additional metabolic targeting is required to improve tumor suppression in non-irradiated and in irradiated tumors.

We found that the MET + SAL combination offers synergistic anti-proliferative and tumor suppressor efficacy in PrCa cells and tumors, at clinically relevant doses, alone and in combination with RT. We used phosphorylated histone-H3 as a marker of DNA replication, which also neatly illustrates chromosomal condensation and cells transitioning through phases of cell cycle (Fig. s2). We observed, that although RT

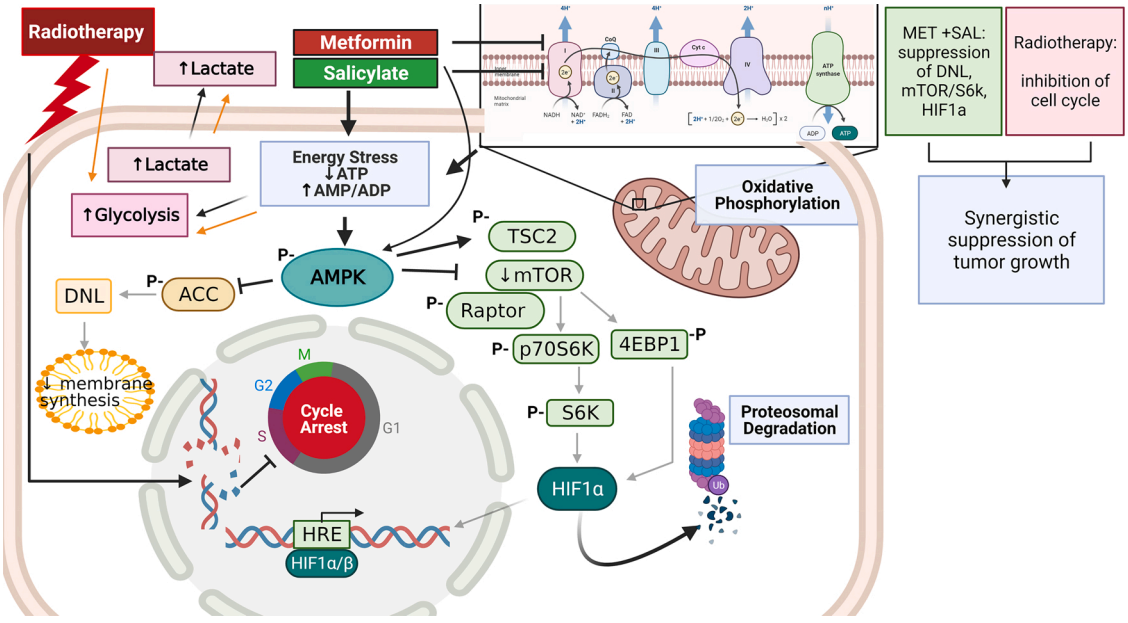

Fig. 6. Model of the mechanism of action of metformin (MET) and salicylate (SAL) in combination with radiotherapy. The results of this work suggest that MET and SAL block mitochondria OxPhos, reduce oxygen consumption and increase extracellular acidification leading to activation of AMPK and induction of downstream pathways. The MET + SAL combination suppresses more effectively lipogenesis and the Raptor-mTOR pathway, mediating an effective blockade of the protein synthesis regulators $p70^{s6k}$ and 4EBP1 and elimination of HIF1α levels. MET + SAL synergize with radiotherapy to provide improved suppression of tumor growth. Created with BioRender.com.

reduced tumor volume significantly, tumor cells surviving six weeks after RT treatment showed average DNA replication rate that was similar to untreated tumors, indicating a need for additional anti-tumor therapy. Consistent with suppression of tumor growth, MET + SAL treatment mediated an impressive reduction of P-H3 positive cells in both non-irradiated and irradiated tumors (Fig. 3) indicating that it could offer the additional anti-tumor activity required to eliminate DNA replication in PrCa tumors.

MET + SAL seems to provide benefit in combination with either conventional (2 Gy) or high dose per fraction (8 Gy) RT. Although, our proliferation assays (Fig. 2) suggested a benefit mainly at lower RT dose fractions (2 Gy), the DNL and immunoblotting analysis (Fig. 5), as well as the *in-vi*vo xenograft results (Fig. 3), illustrated that MET+SAL could improve the effects of high-dose per fraction RT (8–10 Gy) also. Admittedly, here we observed higher than expected response of PrCa xenografts to RT. This made it challenging to demonstrate impressive tumor response to MET and SAL in the irradiated group. Nevertheless, the impact of combined drug treatment was statistically significant in irradiated tumors. Recognizing the limitations of pre-clinical models, we conclude that MET+SAL may be able to improve the response of PrCa to RT of a variety of fractionation schema including conventional-, hypo- and ultra-hypo-fractionated RT, that latter of which is used in stereotactic body RT treatments [38].

The impact of therapeutically relevant MET or SAL doses on mitochondrial OCR was small but, MET + SAL treatment mediated a significant reduction in oxygen consumption rates. This, in combination with a concurrent moderate increase in ECAR, suggests that MET + SAL makes PrCa cells more dependent on glycolysis for their energy metabolism. Interestingly, we detected a significant enhancement of cellular OCR and ECAR with RT treatment alone pointing towards an increased energy generation in irradiated PrCa cells. This is consistent with other reports, which also observed increased mitochondria content in response to RT [39,40]. The adaptation of OCR and ECAR was detected within 48 h suggesting that these alterations can manifest between RT fractions in the clinical setting and could influence response to RT in cells surviving each RT treatment. In irradiated cells, MET+SAL caused improved suppression of OCR, compared to MET or SAL alone, and abolished the OCR gains induced by RT (Fig. 4E). The impact of MET + SAL treatment on OCR/ECAR ratio, an indicator of metabolic stress, was similar in non-irradiated and irradiated cells (Fig. 4E). It is unclear whether the adaptations of OCR and ECAR to RT are beneficial for irradiated cells or whether they contribute to radio-resistance. However, the MET + SAL treatment reversed most efficiently these effects of RT. This could be responsible for the improved RT response seen with this treatment.

Our earlier work showed that the inhibition of PrCa cell growth provided by the combined MET + SAL treatment is mediated by an AMPK-induced suppression of DNL [33]. The efficacy of the MET + SAL combination was blocked in, (i) β1-AMPK subunit knockout mouse embryonic fibroblasts (MEFs), a model with limited AMPK activity[41] and (ii) cells incubated with oleate and mevalonate to reverse the inhibition of DNL [33]. DNL is a key cellular growth function supporting cell membrane and organelle biosynthesis. Consistently, in this study we found that the improved inhibitory phosphorylation of ACC and suppression of DNL by MET + SAL was associated with similar suppression of growth and survival in tissue cultures and greater suppression of tumor growth in xenografts (Figs. 2,3,5).

Protein biosynthesis is regulated by the mTORC1- $p70^{S6k}$/4EPB1 pathway and is vital to cellular growth [42]. Further, HIF1α has an established role in promoting a glycolytic (Warburg type) metabolic phenotype and to stimulate expression of survival and metastasis promoting genes [43], all of which inhibit sensitivity to RT. The inhibition of mTOR signaling by MET + SAL, indicated by the regulation of Raptor, $p70^{S6k}$, S6, 4EBP1 phosphorylation and suppression of HIF1α levels in non-irradiated and irradiated cells, illustrates the significant growth suppressive potential of this drug combination. Combined treatment with MET + SAL was required to effectively reduce the levels of phosphorylated/active forms of $p70^{S6k}$, S6 and 4EBP1 in both non-irradiated cells and in cells treated with conventional (2 Gy) or high dose (8 Gy) RT doses (Fig. 5D,E). HIF1α levels were suppressed by high dose (8 Gy) RT alone but not by 2 Gy. The MET + SAL combination was able to reduce substantially the levels of HIF1a in cells treated with 2 Gy RT, indicating the potential benefit this drug combination could offer if added to human PrCa management with conventional fractionation RT schedules.

Conclusion

Clinically relevant doses of MET and SAL synergize well to provide improved anti-tumor activity in PrCa, compared to each treatment alone. This is associated with improved mitochondria Ox-Phos targeting and suppression of molecular pathways regulating lipid and protein biosynthesis and survival (see Fig. 6). This activity combines well with the cytotoxicity of RT and results in improved response in irradiated PrCa tumors. MET and SAL are widely-used, well-tolerated and highly economical agents, which make them a favorable combination for clinical investigation in PrCa prevention and to improve response to RT. Future studies should also investigate the efficacy of MET+SAL to improve PrCa response to RT + anti-androgen therapy, which is standard of care in high-risk localized PrCa.

CRediT authorship contribution statement

Evangelia E. Tsakiridis: Investigation, Formal analysis, Methodology, Data curation, Writing – original draft. **Lindsay Broadfield:** Investigation, Writing – review & editing. **Katarina Marcinko:** Investigation. **Olga-Demetra Biziotis:** Investigation. **Amr Ali:** Investigation. **Bassem Mekhaeil:** Investigation. **Elham Ahmadi:** Investigation. **Kanwaldeep Singh:** Methodology. **Aruz Mesci:** Methodology, Investigation. **Panayiotis G. Zacharidis:** Investigation. **Alexander E. Anagnostopoulos:** Investigation. **Tobias Berg:** Methodology, Supervision, Funding acquisition, Writing – review & editing. **Paola Muti:** Methodology, Writing – review & editing. **Gregory R. Steinberg:** Conceptualization, Methodology, Supervision, Funding acquisition, Writing – review & editing. **Theodoros Tsakiridis:** Conceptualization, Methodology, Supervision, Project administration, Writing – review & editing, Funding acquisition.

Declaration of Competing Interest

None

Acknowledgments

The authors thank Gabe Menjolian, T. Mathurin, Derek Ribiero and Waqaas Zia from the Radiotherapy Program, Juravinski Cancer Center for the support with cell and animal irradiation.

TB holds the Boris Family Chair in Leukemia and Hematopoietic Stem Cell Translational Research and is supported by the Marta and Owen Boris Foundation, the Canadian Foundation for Innovation and the Ontario Research Fund. GRS is supported by a Diabetes Canada Investigator Award (DI-5-17-5302-GS), a Tier 1 Canada Research Chair and the J Bruce Duncan Endowed Chair in Metabolic Diseases.

PM is now at the Department of Biomedical, Surgical and Dental Sciences, University of Milano, Italy.

Funding

This work was supported by Grants from the Canadian Association of Radiation Oncology (CARO) and the Juravinski Cancer Center Foundation to T.T.; Canadian Institutes of Health Research (CIHR-201709FDN-CEBA-116200) to G.S.; and Hamilton Health Sciences Foundation to T.B.

Supplementary materials

Supplementary material associated with this article can be found, in the online version, at doi:10.1016/j.tranon.2021.101209.

References

[1] D.R. Brenner, H.K. Weir, A.A. Demers, et al., Projected estimates of cancer in Canada in 2020, CMAJ 192 (9) (2020) E199–E205.
[2] R.L. Siegel, K.D. Miller, Jemal a. cancer statistics, 2020, CA Cancer J. Clin. 70 (1) (2020) 7–30.
[3] P. Kupelian, D. Kuban, H. Thames, et al., Improved biochemical relapse-free survival with increased external radiation doses in patients with localized prostate cancer: the combined experience of nine institutions in patients treated in 1994 and 1995, Int. J. Radiat. Oncol. Biol. Phys. 61 (2) (2005) 415–419.
[4] A.L. Zietman, K. Bae, J.D. Slater, et al., Randomized trial comparing conventional-dose with high-dose conformal radiation therapy in early-stage adenocarcinoma of the prostate: long-term results from proton radiation oncology group/american college of radiology 95-09, J. Clin. Oncol. 28 (7) (2010) 1106–1111.
[5] J.R. Molina, Y. Sun, M. Protopopova, et al., An inhibitor of oxidative phosphorylation exploits cancer vulnerability, Nat. Med. 24 (7) (2018) 1036–1046.
[6] M. Troncone, S.M. Cargnelli, L.A. Villani, et al., Targeting metabolism and AMP-activated kinase with metformin to sensitize non-small cell lung cancer (NSCLC) to cytotoxic therapy: translational biology and rationale for current clinical trials, Oncotarget 8 (34) (2017) 57733–57754.
[7] M.R. Owen, E. Doran, A.P. Halestrap, Evidence that metformin exerts its anti-diabetic effects through inhibition of complex 1 of the mitochondrial respiratory chain, Biochem. J. 348 (Pt 3) (2000) 607–614.
[8] B. Viollet, B. Guigas, N. Sanz Garcia, J. Leclerc, M. Foretz, F. Andreelli, Cellular and molecular mechanisms of metformin: an overview, Clin. Sci. (Lond.) 122 (6) (2012) 253–270.
[9] Y. Storozhuk, S.N. Hopmans, T. Sanli, et al., Metformin inhibits growth and enhances radiation response of non-small cell lung cancer (NSCLC) through ATM and AMPK, Br. J. Cancer 108 (10) (2013) 2021–2032.
[10] G.Z. Rocha, M.M. Dias, E.R. Ropelle, et al., Metformin amplifies chemotherapy-induced AMPK activation and antitumoral growth, Clin. Cancer Res. 17 (12) (2011) 3993–4005.
[11] A. Gonnissen, S. Isebaert, C.M. McKee, R.J. Muschel, K. Haustermans, The effect of metformin and GANT61 combinations on the radiosensitivity of prostate cancer cells, Int. J. Mol. Sci. 18 (2) (2017).
[12] H. Kato, Y. Sekine, Y. Furuya, Y. Miyazawa, H. Koike, K. Suzuki, Metformin inhibits the proliferation of human prostate cancer PC-3 cells via the downregulation of insulin-like growth factor 1 receptor, Biochem. Biophys. Res. Commun. 461 (1) (2015) 115–121.
[13] Y. Yang, X.H. Wu, Study on the influence of metformin on castration-resistant prostate cancer PC-3 cell line biological behavior by its inhibition on PLCepsilon gene-mediated Notch1/Hes and androgen receptor signaling pathway, Eur. Rev. Med. Pharmacol. Sci. 21 (8) (2017) 1918–1923.
[14] D. Deng, Y. Yang, X. Tang, et al., Association between metformin therapy and incidence, recurrence and mortality of prostate cancer: evidence from a meta-analysis, Diabetes Metab. Res. Rev. 31 (6) (2015) 595–602.
[15] I.C. Hwang, S.M. Park, D. Shin, H.Y. Ahn, M. Rieken, S.F. Shariat, Metformin association with lower prostate cancer recurrence in type 2 diabetes: a systematic review and meta-analysis, Asian Pac. J. Cancer Prev. 16 (2) (2015) 595–600.
[16] S. Jiralerspong, S.L. Palla, S.H. Giordano, et al., Metformin and pathologic complete responses to neoadjuvant chemotherapy in diabetic patients with breast cancer, J. Clin. Oncol. 27 (20) (2009) 3297–3302.
[17] D. Margel, D.R. Urbach, L.L. Lipscombe, et al., Metformin use and all-cause and prostate cancer-specific mortality among men with diabetes, J. Clin. Oncol. 31 (25) (2013) 3069–3075.
[18] T. Zhang, L. Zhang, T. Zhang, et al., Metformin sensitizes prostate cancer cells to radiation through EGFR/p-DNA-PKCS in vitro and *in vivo*, Radiat. Res. 181 (6) (2014) 641–649.
[19] R.J. Dowling, S. Lam, C. Bassi, et al., Metformin pharmacokinetics in mouse tumors: implications for human therapy, Cell Metab. 23 (4) (2016) 567–568.
[20] K.J. Lipska, C.J. Bailey, S.E. Inzucchi, Use of metformin in the setting of mild-to-moderate renal insufficiency, Diabetes Care 34 (6) (2011) 1431–1437.
[21] T. Sanli, G.R. Steinberg, G. Singh, T. Tsakiridis, AMP-activated protein kinase (AMPK) beyond metabolism: a novel genomic stress sensor participating in the DNA damage response pathway, Cancer Biol. Ther. 15 (2) (2013).
[22] G.R. Steinberg, B.E. Kemp, AMPK in health and disease, Physiol. Rev. 89 (3) (2009) 1025–1078.
[23] M.J. Sanders, P.O. Grondin, B.D. Hegarty, M.A. Snowden, D. Carling, Investigating the mechanism for AMP activation of the AMP-activated protein kinase cascade, Biochem. J. 403 (1) (2007) 139–148.
[24] M. Suter, U. Riek, R. Tuerk, U. Schlattner, T. Wallimann, D. Neumann, Dissecting the role of 5′-AMP for allosteric stimulation, activation, and deactivation of AMP-activated protein kinase, J. Biol. Chem. 281 (43) (2006) 32207–32216.
[25] D. Carling, D.G. Hardie, The substrate and sequence specificity of the AMP-activated protein kinase. phosphorylation of glycogen synthase and phosphorylase kinase, Biochim. Biophys. Acta 1012 (1) (1989) 81–86.
[26] M.D. Fullerton, S. Galic, K. Marcinko, et al., Single phosphorylation sites in Acc1 and Acc2 regulate lipid homeostasis and the insulin-sensitizing effects of metformin, Nat. Med. 19 (12) (2013) 1649–1654.
[27] J.H. Kim, J.M. Park, K. Yea, H.W. Kim, P.G. Suh, S.H. Ryu, Phospholipase D1 mediates AMP-activated protein kinase signaling for glucose uptake, PLoS ONE 5 (3) (2010) e9600.
[28] J. Ye, R.A. DeBose-Boyd, Regulation of cholesterol and fatty acid synthesis, Cold Spring Harb. Perspect. Biol. 3 (7) (2011).
[29] K. Inoki, T. Zhu, K.L. Guan, TSC2 mediates cellular energy response to control cell growth and survival, Cell 115 (5) (2003) 577–590.
[30] D.M. Gwinn, D.B. Shackelford, D.F. Egan, et al., AMPK phosphorylation of raptor mediates a metabolic checkpoint, Mol. Cell 30 (2) (2008) 214–226.
[31] G.R. Steinberg, M. Dandapani, D.G. Hardie, AMPK: mediating the metabolic effects of salicylate-based drugs? Trends Endocrinol. Metab. 24 (10) (2013) 481–487.
[32] S.A. Hawley, M.D. Fullerton, F.A. Ross, et al., The ancient drug salicylate directly activates AMP-activated protein kinase, Science 336 (6083) (2013) 918–922.
[33] A.J. O'Brien, L.A. Villani, L.A. Broadfield, et al., Salicylate activates AMPK and synergizes with metformin to reduce the survival of prostate and lung cancer cells ex vivo through inhibition of de novo lipogenesis, Biochem. J. 469 (2) (2015) 177–187.
[34] L.A. Broadfield, K. Marcinko, E. Tsakiridis, et al., Salicylate enhances the response of prostate cancer to radiotherapy, Prostate 79 (5) (2019) 489–497.
[35] T.C. Chou, P. Talalay, Quantitative analysis of dose-effect relationships: the combined effects of multiple drugs or enzyme inhibitors, Adv. Enzyme. Regul. 22 (1984) 27–55.
[36] M.M. Chitnis, K.A. Lodhia, T. Aleksic, S. Gao, A.S. Protheroe, V.M. Macaulay, IGF-1R inhibition enhances radiosensitivity and delays double-strand break repair by both non-homologous end-joining and homologous recombination, Oncogene 33 (45) (2014) 5262–5273.
[37] S. Supiot, R.P. Hill, R.G. Bristow, Nutlin-3 radiosensitizes hypoxic prostate cancer cells independent of p53, Mol. Cancer Ther. 7 (4) (2008) 993–999.
[38] A.J. Katz, M. Santoro, R. Ashley, F. Diblasio, M. Witten, Stereotactic body radiotherapy for organ-confined prostate cancer, BMC Urol. 10 (2010) 1.
[39] N. Lynam-Lennon, S.G. Maher, A. Maguire, et al., Altered mitochondrial function and energy metabolism is associated with a radioresistant phenotype in oesophageal adenocarcinoma, PLoS ONE 9 (6) (2014), e100738.
[40] T. Yamamori, T. Sasagawa, O. Ichii, et al., Analysis of the mechanism of radiation-induced upregulation of mitochondrial abundance in mouse fibroblasts, J. Radiat. Res. 58 (3) (2017) 292–301.
[41] N. Dzamko, B.J. van Denderen, A.L. Hevener, et al., AMPK beta1 deletion reduces appetite, preventing obesity and hepatic insulin resistance, J. Biol. Chem. 285 (1) (2021) 115–122.
[42] M. Laplante, D.M. Sabatini, mTOR signaling at a glance, J. Cell Sci. 122 (Pt 20) (2009) 3589–3594.
[43] B. Faubert, E.E. Vincent, T. Griss, et al., Loss of the tumor suppressor LKB1 promotes metabolic reprogramming of cancer cells via HIF-1alpha, Proc. Natl. Acad. Sci. U. S. A. 111 (7) (2014) 2554–2559.